Insights and Innovations in Structural Engineering, Mechanics and Computation – Zingoni (Ed.)
© 2016 Taylor & Francis Group, London, ISBN 978-1-138-02927-9

A load-displacement based approach to assess the bearing capacity and deformations of mono-bucket foundations

M.J. Vahdatirad, A. Troya Diaz & S. Nielsen
Universal Foundation A/S, Aalborg, Denmark

L.B. Ibsen, L.V. Andersen & S. Firouzianbandpey
Department of Civil Engineering, Aalborg University, Aalborg, Denmark

D.V. Griffiths
Department of Civil and Environmental Engineering, Colorado School of Mines, Golden, CO, USA

ABSTRACT: It is now accepted that a larger effort must be made in order to optimize the design so that offshore wind turbines can be competitive with the other energy resources. In this regard, mono-buckets are known as a cost-effective offshore foundation solution. In the current study, a load–displacement based approach is introduced to assess the bearing capacity as well as the deformation of a mono-bucket foundation subjected to combined loading. A *p-y* curve developed for the bucket foundation is used to quantify the lateral soil response around the foundation. A numerical routine to set up the model and run the calculations is proposed. The model is validated, and its accuracy is analyzed, by comparison with field test results for a bucket foundation installed in silty, sandy soil.

1 INTRODUCTION

Within the oil and gas industry, suction caissons are known to be a cost-effective solution for jacket structures in deep waters. Nowadays, a similar concept, the so-called mono-bucket, has been invented and adopted for wind-turbine foundations. The advantages of this concept are ease and speed of the installation, providing higher stiffness and exclusion of a transition piece (Ibsen 2008). Furthermore, being located in the skirted-foundation category provides mono-buckets with the advantages of gravity based foundations by having a big diameter and monopiles by having a skirt or frictional area. As a result, mono-buckets are lighter, faster to install and, hence, more cost efficient than other solutions.

The application of bucket foundation for offshore wind turbines has already been investigated abundantly and its efficiency has been verified (Byrne 2000, Feld 2001, Ibsen *et al.* 2004, Houlsby *et al.* 2005, Houlsby *et al.* 2006, Ibsen 2008). Despite the advantages, there is no standard routine to design the foundation, especially for assessing the bearing capacity and deformations due to the complexity in the failure mechanisms. However, there are several semi-analytical approaches based on experimental and numerical studies to assess the bearing capacity of the buckets as well as skirted foundations. As an example, Byrne *et al.* (2003) conducted a series of laboratory tests in order to assess the vertical and moment bearing capacity of the shallow skirted foundation mounted in sand. A comparison was made between the laboratory test results and simple theoretical expressions based on standard bearing capacity formulae. Gourvenec and Barnett (2015) proposed a closed-form expression in order to estimate the undrained bearing capacity of the skirted foundation. They provided three-dimensional (3D) failure envelopes such that the bearing capacity under the general combined loading can be predicted for a range of embedment ratios. In a similar study, Larsen *et al.* (2013) and Ibsen *et al.* (2014) suggested a modified expression in order to quantify the combined bearing capacity of the bucket foundation in sand. The modified expression was interpreted based on several experimental studies of the bucket subjected to combined loading.

All the mentioned methods are proposed to analyze the bucket foundation only for the ultimate limit state and bounded with assumptions such as homogenous soil. This makes the design of buckets for complex situations, *e.g.* layered soils, difficult. Further, a deformation analysis cannot be performed with the mentioned semi-analytical techniques.

Therefore, numerical analyses and considering constitutive soil models are typically suggested

for the more sophisticated cases. However, these calculations are normally time consuming and therefore inefficient for preliminary or conceptual design, especially when 3D simulation with an advanced soil model is performed. Hence, using a fast and sufficiently accurate method, eliminating the complexity of detailed numerical calculation and with the ability of modeling the layered soil and performing deformation analysis, is highly demanded in the preliminary design phases.

The main objective of the current study is to establish a fast and relatively accurate method to estimate the bearing capacity and deformations of mono-buckets, *i.e.* a model that can be applied in the ultimate limit state (ULS) as well as the serviceability limit state (SLS). The idea comes from the load–displacement method, the so-called Winkler model, which is proposed by standards (American Petroleum Institute 2012, Det Norske Veritas 2013) as a well-accepted method for pile foundations. In this model for mono-buckets, the soil–structure interaction is introduced by nonlinear springs acting along the skirt and beneath the lid of the foundation in different directions. The bucket itself is modeled as a frame structure. The model employs formulations for the stiffness of the springs similar to those proposed for *p-y*, *t-z* and *q-w* curves for pile foundations. However, special *p-y* curves are utilized for mono-buckets, since the curves proposed for pile foundations are not representative for buckets given their larger diameter and shorter skirt length.

The *p-y* curves employed in the current study were developed from a set of 3D Finite Element (FE) calculations for the bucket in sand (Knudsen *et al.* 2015). The numerical analyses were conducted for different bucket geometries and for a range of soil stiffness and strength properties. The Hardening Soil Small Strain (HSsmall) model available in Plaxis (2015) has been employed to capture more realistically the response of the bucket in 3D. Hence, more accurate *p-y* load–displacement curves are obtained. In the current model, shear resistance at the bottom of the bucket is taken into account since it has a big impact on the bearing capacity and stiffness due to a large resisting area beneath the foundation. The results from this model have been checked and validated by comparison with results from a field test carried out with a large model of a bucket installed in sandy soil. The comparisons suggest an acceptable match between the proposed model and the test.

2 LOAD-DISPLACEMENT MODEL

As embedded foundations, mono-buckets are subject to soil pressure around the skirt of the bucket. Hence, a concept similar to that for embedded foundations can be implemented for the lateral reactions along the embedded part of the bucket. In this regard, *p-y* load–displacement curves can be assigned as spring properties to simulate the soil stiffness around the bucket (Fig. 1). However, standard *p-y* curves suggested for pile foundations (American Petroleum Institute 2012, Det Norske Veritas 2013) might not be representative for the buckets with very small aspect ratio, *L*/*D* (*i.e.*, length divided by diameter). Instead, a *p-y* curves calibrated to the lateral soil mobilization and deformation mechanisms of bucket foundations must be applied. In addition to the lateral response, the bucket also resists an applied moment by vertical sleeve reaction along the skirt. This can be modeled by *t-z* load–displacement curves as illustrated in Figure 1. Furthermore, the bucket foundation is typically assumed to be plugged (Randolph & Gourvenec 2011), and therefore the sleeve resistance is limited to the outside area of the skirt. However, since the bucket is plugged, vertical and shear/sliding resistance should be considered at the base due to the large cross-sectional area of the soil plug inside the foundation. This contribution to the resistance can be quantified with *q-w* and *sliding* springs as presented in Figure 1.

2.1 *Lateral resistance*

As mentioned above, calibrated *p-y* curves are used in order to assess the lateral response due to the earth pressure around the foundation. In this study, *p-y* curves developed for a bucket mounted in sandy soil are used, see Equation 1 (Knudsen *et al.* 2015). In this equation, mobilized lateral soil resistance per unit length, *p*, is defined as a function of soil properties and displacement, *y*, normalized with the bucket diameter, *D*, and given as

$$\frac{p}{p_R} = \beta_1 \cdot \tanh(\beta_2 \frac{y}{D}) + \beta_3 \cdot \tanh(\beta_4 \frac{y}{D}) + \frac{K_0}{K_P - K_A}, \quad (1)$$

where K_0, K_A and K_P are coefficients of the lateral earth pressure at rest, active and passive conditions respectively, and p_R is the Rankine earth pressure per unit length:

$$p_R = \sigma'_{v0} \cdot D \cdot (K_P - K_A), \quad (2)$$

where σ'_{v0} = effective overburden pressure.

In Equation 1, β_1 to β_4 are fitting coefficients controlling the curvature and ultimate pressure for the *p-y* curves. These coefficients are obtained from Equations 3 and 4 (Knudsen *et al.* 2015):

$$\beta_1 + \beta_3 = 0.041 \frac{\varphi'}{L} + 2.05, \quad (3a)$$

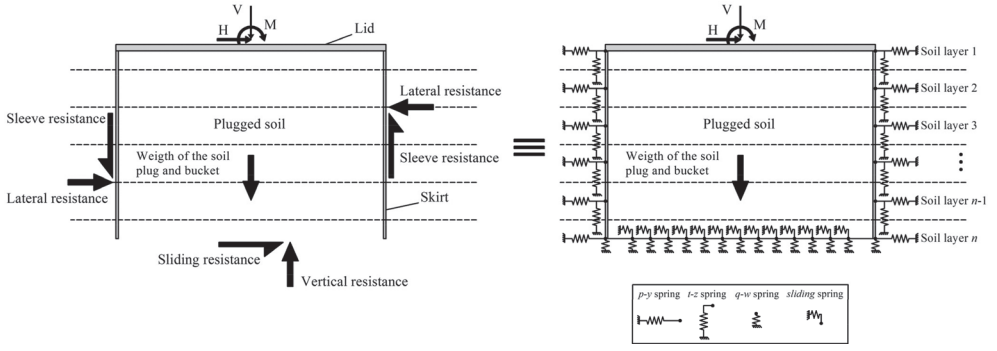

Figure 1. Mono-bucket model: Conceptual sketch of loads and resistances (left); equivalent frame supported by Winkler springs for the soil-structure interaction (right). V, H and M are vertical, horizontal and overturning moment loads respectively.

$$\beta_1\beta_3 = 0.107\frac{\varphi'}{L} + 0.56, \tag{3b}$$

$$\beta_2 + \beta_4 = 8.9(\frac{\varphi'}{L})^2 - 13.12\frac{\varphi'}{L} + 66.24, \tag{4a}$$

$$\beta_2\beta_4 = 936.50(\frac{\varphi'}{L})^2 - 4579\frac{\varphi'}{L} + 5989, \tag{4b}$$

where φ' is the effective friction angle of sand and L is the skirt length of the bucket. Angles and lengths must be given in degrees and meters, respectively.

2.2 *Sleeve resistance*

The standard *t-z* curves for sand suggested by American Petroleum Institute (2012) are used as presented by the tabulated values in Table 1. In this table, the relation between skin displacement, z, and mobilized unit skin friction, t, is defined. Notice that t is normalized with respect to the maximum unit skin friction, t_{max}, obtained from Equation 5 (American Petroleum Institute 2012):

$$t_{\max} = K \cdot \sigma'_{v0} \cdot \tan\delta \le f_1, \tag{5}$$

where K is the coefficient of lateral earth pressure, $\tan\delta = 2/3 \tan\varphi'$ is the effective wall friction, and f_1 is the limiting unit skin friction corresponding to δ, see Table 2.

2.3 *Bottom, vertical and sliding resistance*

In order to obtain the vertical and sliding resistances, standard *q-w* curves (American Petroleum Institute 2012) are used to model the response of the springs attached to the base of the soil plug and foundation (see *q-w* and sliding springs in Figure 1). Table 3 presents the relation between the normalized tip displacement, w/D, and the mobilized end-bearing capacity, q_{end}. Here, q_{end} is normalized with respect to the maximum end-bearing capacity, q_b, given by Equation 6 for vertical resistance (American Petroleum Institute 2012) and Equation 7 for sliding resistance in sand (Det Norske Veritas 2013):

$$q_b = N_q \cdot \sigma'_{v0} \text{ (vertical end bearing)}, \tag{6}$$

where N_q is the end-bearing capacity factor obtained from Table 2;

$$q_b = \sigma'_{v0} \cdot \tan\varphi' \text{ (sliding end bearing)}. \tag{7}$$

2.4 *Numerical scheme*

An FE scheme is employed to model the bucket–soil interaction represented by the springs. The load–displacement curves defined in the previous

Table 1. *t-z* curve for sandy soil.

z [mm]	t/t_{max} [–]
0.00	0.00
2.50	1.00
⊥	1.00

Table 2. Limiting unit skin friction, f_1, and end bearing capacity factor, N_q, for sandy soils.

δ [o]	f_1 [–]	N_q [–]
15	0.48	8
20	67	12
25	81	20
30	96	40
35	115	50

Table 3. Load-displacement values for *q-w* and *sliding* springs.

w/D [–]	q_{end}/q_b [–]
0	0
0.002	0.25
0.013	0.5
0.042	0.75
0.073	0.9
0.1	1

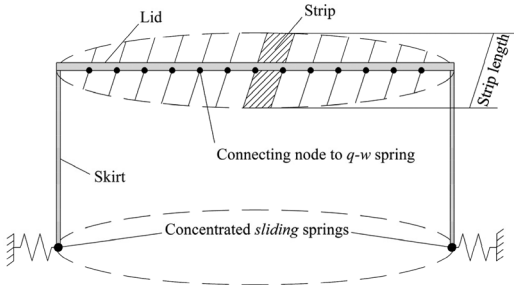

Figure 2. Discretization of the bucket lid: Nodes and strips.

sections are used to calculate the stiffness of the different springs. The real bucket is a three-dimensional shell structure. However, the load–displacement curves described above are calibrated from a 3D FE model such that the bucket should be modeled as a plane frame structure. The frame structure is discretized into a number of two-node beam elements as illustrated in Figure 1. Each node has three Degrees of Freedom (DOFs). The bending and axial stiffnesses of the frame are chosen such that the global response of the 2D model will match the response of the cylindrical bucket in terms of overall flexibility. Because of this approach, the considered 2D model does not provide any meaningful insight into the stresses that will occur in the 3D steel structure. In any case, the bucket behaves rigid relatively to the soil and internal deformation and stresses in the structure are not the main interest in this study.

To simulate the lateral and sleeve stiffness related to the translational DOF, *p-y* and *t-z* springs (acting per unit length of the skirt) are attached to the nodes in the skirt of the bucket. The influence of *sliding* springs is integrated over the base of the soil plug and foundation, and half of the stiffness is transferred to either of the bottom nodes in the skirts (see Figure 2). In the 3D structure, a gradual transition from base shear into normal traction on the inside of the skirt occurs; but given the high stiffness of the structure, the abovementioned approach is considered adequate. The *q-w* springs are transferred from the base of the soil plug to the lid, thus disregarding the flexibility of the soil plug in the vertical direction. Hence, no discretization is required for the soil plug or its base. The springs at the bottom of the lid do not represent the same area since the lid is circular. Therefore, the contact area is discretized into a number of strips as shown in Figure 2. The length of each strip is multiplied by the stiffness of the spring connected to the corresponding node in order to account for the correct stiffness contribution.

Once the connectivity of the soil springs and structural beam elements is defined for each DOF, the stiffness matrix of the entire soil–structure system is constructed. Moreover, the vector describing the external forces applied in each DOF is constructed for the soil–structure system. In this vector, the vertical, horizontal and moment loads are assigned, respectively, to the vertical, horizontal and rotational DOF of the node located in the center of the lid. The loads are applied incrementally.

When the stiffness matrix and force vector have been constructed for each loading step, the displacement vector can be obtained. It is noted that the soil-spring stiffness is nonlinear as described in the previous sections. Therefore, an iterative process is considered, in which a predefined displacement vector is used to obtain the secant soil stiffness for each loading step. The predefined displacement for each step is the solution provided from the previous step. Zero displacements are used to find the initial soil stiffness for the first loading step. The calculation is terminated for each loading step when the absolute difference between the displacements obtained in two successive iterations is less than a predefined error. Figure 3 illustrates the calculation procedure for the described numerical scheme.

3 VALIDATION OF THE MODEL

Validation of the model is performed by comparing the computed moment–rotation curves with field test results for a foundation installed in sandy soil and subjected to combined loading.

3.1 *Field test*

The field test was performed in the northern part of Jutland in Denmark (Fig. 4) in the fall of 2002 as a part of a research program. The results were provided by Universal Foundation A/S. The experiment was conducted on a bucket with a diameter of 2 m, a skirt length of 2 m, and a skirt thickness of 15 mm. The lid of the bucket was made of a 12 mm thick reinforced steel plate (Fig. 5). The site consists

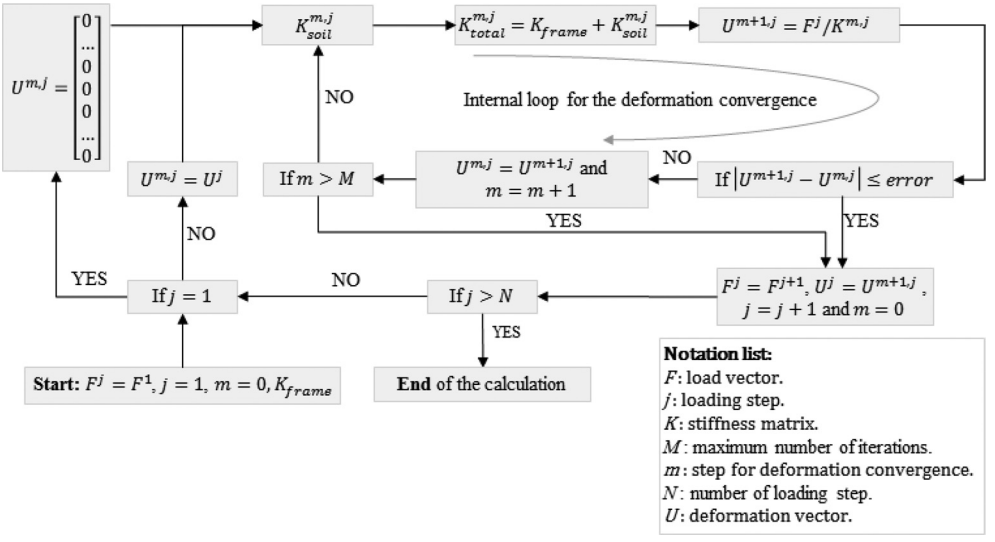

Figure 3. Calculation procedure proposed for the numerical load-displacement model.

Figure 4. Location where the field test was conducted.

Figure 5. Steel bucket used for the experiments. (The two steel structures at each side of the bucket are used to measure the displacements during loading).

of a reservoir of saturated silty sand. The bucket was installed and left with a tower on top of it for almost one year and thereafter loaded until failure.

Figure 6 shows the general test setup used during the combined loading phase. The bucket was loaded with the combination of a moment, horizontal and vertical force. The vertical force stemmed from the self-weight of the bucket and the tower including the equipment attached to it, can provide a maximum vertical force of 130 kN. The horizontal force was applied by pulling a steel wire connected to the tower at the height *h* above the bucket foundation lid. The steel wire was loaded with a hydraulic piston attached to a loading tower founded on three concrete blocks. The height of the impact, which was equal to 19.1 m, has induced a moment on the foundation.

3.2 *Soil profile*

Four CPT tests were performed prior to the installation of the bucket in the field. These were

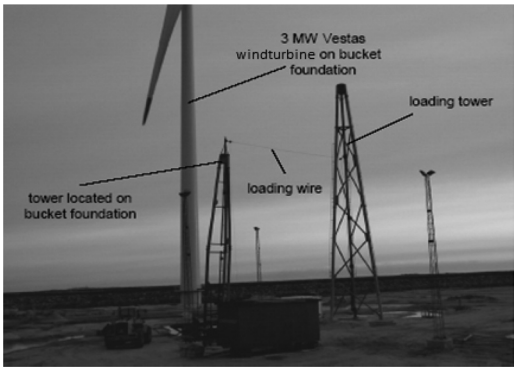

Figure 6. Test setup during combined loading of the bucket.

performed at a distance of 0.5 m from the point where the center of the bucket was to be installed. From the CPT results and based on the physical evidence from the reservoir, a soil profile is established and the different parameters needed for the load–displacement model are interpreted. The soil profile consists of a homogeneous layer of silty sand. The total unit weight of the soil is derived from the CPT measurements based in the correlation proposed by Robertson & Cabal (2010) which had been shown to give fair estimates of the soil unit weight. The strength of the soil profile is described by the effective friction angle of the homogeneous layer which is derived using an empirical relation proposed by Jensen (2015). This relation provides a proper estimate of the effective friction angle of silty sand, since it takes into account the mineralogy, relative density, dilatancy potential, effective stress level and silt content. The state and strength parameters of the assumed homogeneous silty sand profile are listed in Table 4.

3.3 *Results and discussion*

From the moment-rotation curves presented for the field test and the load-displacement model (Fig. 7), it is demonstrated that the ultimate bearing capacity of the bucket foundation is well predicted by the load-displacement model. However, the small-strain response of the foundation in the field test is seen to behave stiffer than the one predicted by the model. In contrast with the results from the field test, the model reduces stiffness more abruptly after a certain level of deformation (around 0.25 degrees). This could be due to fitting coefficients, β_2 and β_4 in Equation 4, controlling the shape of the curve in the calibrated *p-y* model. Therefore, these parameters can be calibrated using the test results to provide an analogous response.

Table 4. Soil parameters for the load–displacement model.

Total soil unit weight γ' [kN/m^3]	Effective friction angle φ' [°]
19	32.5

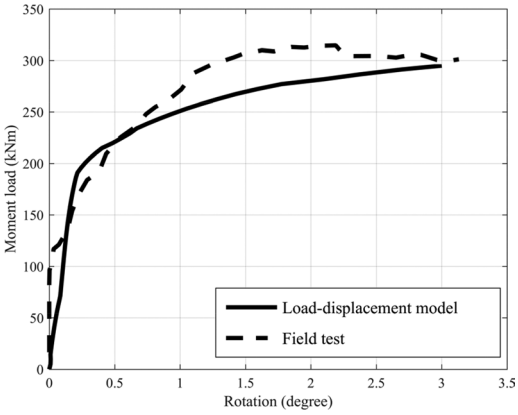

Figure 7. Comparison of the moment-rotation curve from the load-displacement model and the field test.

4 CONCLUSION

A load-displacement based model has been used to assess the bearing capacity and deformations of mono-bucket foundation under combined loading. The model includes the lateral response in sandy soils by the use of *p-y* curves that had been developed explicitly for bucket foundations by means of 3D FEM modeling. Since the soil inside the bucket is considered plugged, the model considers only the exterior skirt for the frictional resistance. Furthermore, it also includes the vertical and sliding resistance at the bottom of the bucket and soil plug.

A numerical scheme comparable to the ones in FEM codes has been utilized to implement the load-displacement model in order to obtain the response of the structure interacting with soil due to combined loading. The load–displacement model has been validated by the results from a field test performed with a 2 by 2 m bucket in a reservoir containing saturated silty sand. A reasonable match between the field test results and the proposed model in this study has been found, specifically for the bearing capacity of the bucket. Calibration of the fitting coefficients that control the shape of the *p-y* load–displacement curves could provide a closer match of the calculated

response to the shape of the moment–rotation curve obtained from the field test.

REFERENCES

American Petroleum Institute 2012. Recommended Practice for Planning, Designing and Constructing Fixed Offshore Platforms–Working Stress Design.

Byrne, B. 2000. *Investigation of suction caissons in dense sand*. Ph.D. thesis. University of Oxford.

Byrne, B., Villalobos, F., Houlsby, G. & Martin, C. 2003. Laboratory testing of shallow skirted foundations in sand. In *International Conference on Foundations; Proc. British Geotechnical Association*. Dundee: pp. 161–173.

Det Norske Veritas 2013. DNV-OS-J101 - Design of Offshore Wind Turbine Structures.

Feld, T. 2001. Suction buckets, a new innovative foundation concept, applied to offshore wind turbines. Ph.D. thesis. Aalborg University, Denmark.

Gourvenec, S. & Barnett, S. 2011. Undrained failure envelope for skirted foundations under general loading. *Géotechnique*, 61(3): pp. 263–270.

Houlsby, G., Ibsen, L. & Byrne, B. 2005. Suction caissons for wind turbines. In *Frontiers in Offshore Geotechnics: ISFOG*. Perth, WA, Australia: pp. 75–93.

Houlsby, G., Kelly, R., Huxtable, J. & Byrne, B. 2006. Field trials of suction caissons in sand for offshore wind turbine foundations. *Géotechnique*, 56(1): pp. 3–10.

Ibsen, L.B. 2008. Implementation of a new foundation concept for offshore wind farms. In *Proceedings of the 15th Nordic Geotechnical Meeting*. Norway: pp. 19–33.

Ibsen, L.B. Larsen, K.A. & Barari, A. 2014. Calibration of failure criteria for bucket foundations on drained sand under general loading. *Journal of Geotechnical and Geoenvironmental Engineering*, 140(7): pp. 1–16.

Ibsen, L., Schakenda, B. & Nielsen, S. 2004. Development of the bucket foundation for offshore wind turbines, a novel principle. In *Gigawind-Symposium Offshore-Windenergie, Bau-und umwelttechnische Aspekte*. Hannover.

Jensen, B.C., 2015. *Teknisk Ståbi*: Nyt Teknisk Forlag.

Knudsen, B.S., Østergaard, M.U., Ibsen, L.B. & Clausen, J. 2015. Determination of *p-y* Curves for Bucket Foundations in Sand Using Finite Element Modeling. In *Frontiers in Offshore Geotechnics iii Proceedings of the Third International Symposium on Frontiers in Offshore Geotechnics (isfog 2015), Oslo, Norway, 10–12 June 2015*: pp. 343–348.

Larsen, K., Ibsen, L. & Barari, A. 2013. Modified expression for the failure criterion of bucket foundations subjected to combined loading. *Canadian Geotechnical Journal*, 50(12): pp. 1250–1259.

Plaxis 2015. Brinkgreve, R.B.J., Kumarswamy, S. & Swolfs, W.M. (Edtitors). Plaxis bv. The Netherlands.

Randolph, M. & Gourvenec, S. 2011. *Offshore geotechnical engineering*: CRC Press.

Robertson, P.K. & Cabal, K.L. 2010. Estimating soil unit weight from CPT. In *2nd international symposium on cone penetration testing, CPT*. Hungtington Beach, CA.